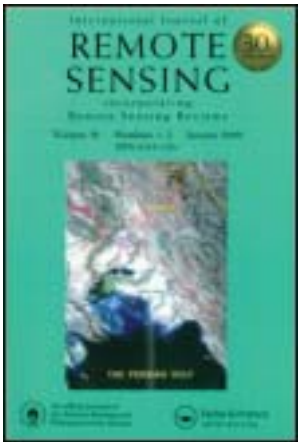

International Journal of Remote Sensing

Publication details, including instructions for authors and subscription information:
http://www.tandfonline.com/loi/tres20

Classification of dust days by satellite remotely sensed aerosol products

M. Sorek-Hamer [a] , A. Cohen [b] , R.C. Levy [c] , B. Ziv [d] & D.M. Broday [a]

[a] Civil and Environmental Engineering, Technion, Haifa, Israel

[b] Industrial and Management Engineering, Technion, Haifa, Israel

[c] NASA, Goddard Space Flight Center, Greenbelt, MD, USA

[d] The Open University of Israel, Raanana, Israel

Version of record first published: 18 Dec 2012.

To cite this article: M. Sorek-Hamer , A. Cohen , R.C. Levy , B. Ziv & D.M. Broday (2013): Classification of dust days by satellite remotely sensed aerosol products, International Journal of Remote Sensing, 34:8, 2672-2688

To link to this article: http://dx.doi.org/10.1080/01431161.2012.748991

International Journal of Remote Sensing
Vol. 34, No. 8, 20 April 2013, 2672–2688

Taylor & Francis
Taylor & Francis Group

Classification of dust days by satellite remotely sensed aerosol products

M. Sorek-Hamer[a], A. Cohen[b], R.C. Levy[c], B. Ziv[d], and D.M. Broday[a]*

[a]*Civil and Environmental Engineering, Technion, Haifa, Israel;* [b]*Industrial and Management Engineering, Technion, Haifa, Israel;* [c]*NASA, Goddard Space Flight Center, Greenbelt, MD, USA;* [d]*The Open University of Israel, Raanana, Israel*

(*Received 21 May 2012; accepted 23 August 2012*)

Considerable progress in satellite remote sensing (SRS) of dust particles has been seen in the last decade. From an environmental health perspective, such an event detection, after linking it to ground particulate matter (PM) concentrations, can proxy acute exposure to respirable particles of certain properties (i.e. size, composition, and toxicity). Being affected considerably by atmospheric dust, previous studies in the Eastern Mediterranean, and in Israel in particular, have focused on mechanistic and synoptic prediction, classification, and characterization of dust events. In particular, a scheme for identifying dust days (DD) in Israel based on ground PM_{10} (particulate matter of size smaller than 10 μm) measurements has been suggested, which has been validated by compositional analysis. This scheme requires information regarding ground PM_{10} levels, which is naturally limited in places with sparse ground-monitoring coverage. In such cases, SRS may be an efficient and cost-effective alternative to ground measurements. This work demonstrates a new model for identifying DD and non-DD (NDD) over Israel based on an integration of aerosol products from different satellite platforms (Moderate Resolution Imaging Spectroradiometer (MODIS) and Ozone Monitoring Instrument (OMI)).

Analysis of ground-monitoring data from 2007 to 2008 in southern Israel revealed 67 DD, with more than 88% occurring during winter and spring. A Classification and Regression Tree (CART) model that was applied to a database containing ground monitoring (the dependent variable) and SRS aerosol product (the independent variables) records revealed an optimal set of binary variables for the identification of DD. These variables are combinations of the following primary variables: the calendar month, ground-level relative humidity (RH), the aerosol optical depth (AOD) from MODIS, and the aerosol absorbing index (AAI) from OMI. A logistic regression that uses these variables, coded as binary variables, demonstrated 93.2% correct classifications of DD and NDD. Evaluation of the combined CART–logistic regression scheme in an adjacent geographical region (Gush Dan) demonstrated good results. Using SRS aerosol products for DD and NDD, identification may enable us to distinguish between health, ecological, and environmental effects that result from exposure to these distinct particle populations.

1. Introduction

Several regions are known to be sources for dust resuspension, including northeastern and central Asia, north Africa, Saudi Arabia, Sudan, Chad, and central Australia (Dayan

*Corresponding author. Email: dbroday@tx.technion.ac.il

ISSN 0143-1161 print/ISSN 1366-5901 online

http://dx.doi.org/10.1080/01431161.2012.748991
http://www.tandfonline.com

et al. 2007; Ganor et al. 2010; Ochirkhuyag and Tsolmon 2008; Washington et al. 2003). Airborne dust has a wide environmental impact, including effects on visibility, radiative forcing, and the Earth's energy balance (Goudie and Middleton 2006; Washington et al. 2003). Being affected considerably by atmospheric dust, previous studies in the Eastern Mediterranean, and in Israel, in particular, focused on mechanistic (Alpert et al. 2002) and synoptic (Alpert et al. 2004) identification, characterization, prediction, and classification of dust events. The spectrum of tools used in these studies include mineralogical and chemical characterization of dust particles (Erel et al. 2006; Ganor, Stupp, and Alpert 2009; Kalderon-Asael et al. 2009), estimation of particle transboundary transport and fate (Rudich et al. 2008), and analysis of satellite observations (Carmona and Alpert 2009). Days heavily affected by dust, termed hereafter dust days (DD), were found to occur during certain synoptic patterns (Alpert et al. 2004; Dayan et al. 2007) and to be characterized by specific meteorological conditions (Ganor et al. 2010). These conditions carry with them information regarding the origin of the dust and therefore its related attributes, which can affect the health of the exposed individuals. In particular, during their transport, dust particles can absorb airborne pollutants such as metals and volatile organic compounds (Erel et al. 2006; Falkovich et al. 2004) that modify their mineral composition and consequently their supposedly harmlessness nature. Indeed, the literature on health effects from exposure to dust is inconsistent. Whereas some studies report non-detrimental effects from exposure to crustal (Laden et al. 2000) and dust (Prospero et al. 2008; Schwartz et al. 1999) particles, other studies report clear evidence of adverse health effects (cf. Jiménez et al. 2010; Lipsett et al. 2006; Middleton et al. 2008).

To date, identification and characterization of DD in Israel have been based mainly on ground particulate matter (PM) observations and compositional analysis (Dayan et al. 2007; Ganor, Stupp, and Alpert 2009). Following Kaufman et al. (2005), who introduced the use of satellite-borne data to distinguish dust aerosols over the ocean, the last decade has seen considerable progress in using satellite remote sensing (SRS) for retrieving reliable data on dust aerosols (cf. Christopher and Jones 2010) and for developing different techniques for utilizing data from the Moderate Resolution Imaging Spectroradiometer (MODIS) and Ozone Monitoring Instrument (OMI) for dust detection. Examples include the use of satellite data and imagery for studying dust events and their broad environmental effects over the Australian (Baddock, Bullard, and Bryant 2009) and Indian (Badarinath et al. 2010) subcontinents, the Persian Gulf, northwestern China, and the USA (Huang et al. 2010). Environmental health studies, however, mostly use risk metrics that are based on ground air quality data. To overcome the sparse and heterogeneous spatial distribution of ground-monitoring stations, satellite-borne observations of the aerosol optical depth (AOD) through atmospheric columns have been suggested as a proxy of ground-level PM. Assessing the relationships between AOD and surface PM is an active research area (e.g. Engel-Cox et al. 2004; Hutchison, Smith, and Faruqui 2005; Lee et al. 2011; Paciorek et al. 2008; Van Donkelaar et al. 2010), which has recently been utilized also in epidemiological studies (Hu 2009; Hu and Rao 2009). In particular, the use of AOD retrievals from the MODIS instruments on board Terra and Aqua polar-orbiting satellites for environmental health applications is currently explored due to the AOD data spatial coverage, temporal resolution (almost daily global coverage), and availability. Satellite imagery is a useful tool for identifying specific aerosol events, such as large biomass fires, volcanic ash, smoke, and thick haze (Hoff and Christopher 2009; Martin 2008; Van Donkelaar et al. 2011). However, an efficient DD identification scheme for analysing more than a few specific days/events, e.g. for comprehensive environmental health studies, has not been explored to

date. This study focuses on developing a model for retrospective identification of days with considerable dust concentrations using almost solely satellite-borne aerosol products.

A scheme for identifying DD in Israel, based on ground PM_{10} (particulate matter of size smaller than 10 μm) measurements, was suggested and validated by PM compositional analysis by Ganor, Stupp, and Alpert (2009). Their criterion to assess, retrospectively, whether a given day was a dust day (a day characterized by a dominant particulate mineral fraction) is if at least three consecutive hours (six successive half-hourly readings) of PM_{10} records were above 100 μm m^{-3}, with the highest value above 180 μm m^{-3}. Naturally, this scheme requires information on ground PM_{10} concentrations and is clearly limited, therefore, to places with ground-monitoring coverage. For example, ground PM monitoring in urban areas in Israel is fairly dense, with an average interstation separation of ~5 km, whereas in rural areas it is rather sparse (Figure 1). In such areas, it would have been useful if SRS aerosol products could be used to identify DD and non-DD (NDD). Discriminating between these two populations has merit for environmental health studies due to the potentially distinct toxicity of the particles and for air quality management when abatement measures are sought as a response to recurrent exceedances. In this work, we present a scheme that may enable epidemiologists, environmental scientists, and ecologists to explore the distinct effects of dust and non-dust particles on expanded temporal scales.

2. Data

2.1. Ground observations

Half-hourly concentrations of PM_{10} and $PM_{2.5}$ (particulate matter of size smaller than 2.5 μm) from 2007 to 2008, gathered by the regional air quality monitoring network in southern Israel (Figure 1), were used. The typical instrument error is ±1% (Yuval and Broday 2006). The PM_{10} data were used for (a) identifying DD and NDD in the training sets and (b) evaluating the results of the logistic regression model when it operated on the

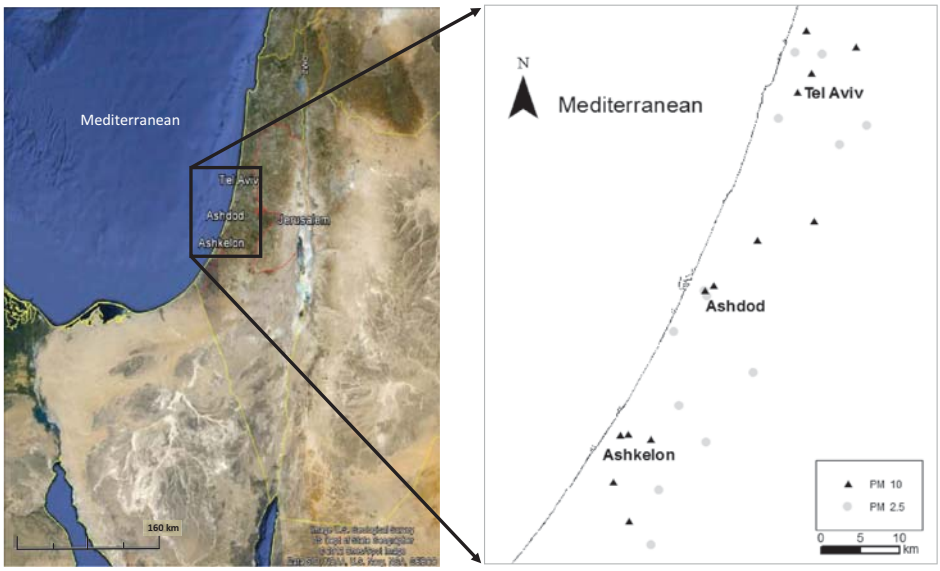

Figure 1. Locations of PM monitoring stations in the study area in southern and central Israel.

test data sets (see Section 3). Reliable relative humidity (RH) data were obtained from a ground meteorological station situated near one of the air quality monitoring stations. The RH data were used at the model evaluation stage (see Section 3). Characteristics of all the DD observed during the study period were studied by applying Alpert et al.'s (2004) semi-objective classification of daily synoptic patterns based on the National Centers for Environmental Prediction National Center for Atmospheric Research (NCEP/NCAR) reanalysis data and by a careful inspection of back-trajectories of air masses using the Hybrid Single Particle Lagrangian Integrated Trajectory (HYSPLIT) model (http://ready.arl.noaa.gov).

2.2. Satellite data

The Terra and Aqua satellites pass over the study area (southern Israel: 31.52° N−31.91° N, 34.5° E−34.85° E) between 09:30 and 11:30 and 12:00 and 14:00 UTC, respectively. MODIS collection 5.1 data (Levy et al. 2009; http://modis-atmos.gsfc.nasa.gov) from 1 January 2007 to 31 December 2008 from both platforms were used. The MODIS products that were used include (a) the AOD at 550 nm, retrieved using the operational dark target (DT) algorithm, (b) the Ångström exponent (AE), derived from the DT–AOD retrievals at 470 and 670 nm over the land, and (c) the single scattering albedo (SSA, the ratio of the aerosol scattering to its extinction coefficients) at 470 nm. Typically, for a given pair of wavelengths, the AE decreases as the particle size increases and takes values ranging from more than 1.5 for fine particles like those formed during combustion processes to nearly zero for coarse dust particles (Kaskaoutis et al. 2007). Similarly, the SSA has been used as a key parameter for defining the aerosol optical properties and for classification of aerosol types (Meloni et al. 2006). However, as will be shown, due to poor availability and small variability of the SSA in this study, it turned out to be inadequate for DD identification.

MODIS Level 2 aerosol products with a spatial (grid) resolution of 10 km × 10 km and quality flags of 'good' and 'very good' (QA = 2 and QA = 3, respectively) were used. Ichoku et al. (2002) suggested that 5 pixel × 5 pixel averaging of MODIS AOD is spatially correlated with hourly averages of AOD, τ, observed by ground sunphotometers (AERONET), with a global uncertainty of the MODIS DT–AOD relative to the AERONET AOD of $\Delta\tau = \pm(0.05 + 0.15\tau)$ (Levy et al. 2010). Since the correlation coefficients between the AERONET AOD from the Ness-Ziona site, Israel, and the MODIS DT–AOD from Aqua and Terra were 0.87 and 0.89, respectively, and as the expected AOD error was within the global uncertainty range, the quality of the MODIS DT–AOD used in this study was confirmed. Furthermore, based on 7 year data, Kaufman et al. (2000) concluded that the aerosol products from MODIS 'instantaneous' overpass highly correlate with the daily average AOD. Hence, the daily average aerosol products were used throughout this study.

OMI, on board Aura, measures the Earth reflectance spectra in both visible (VIS) and ultraviolet (UV) (270–500 nm) spectral bands and can distinguish between UV-absorbing aerosols, such as desert dust, and weakly UV-absorbing aerosols and clouds (Kazadzis et al. 2009; Stammes and Noordhoek 2002). The aerosol absorbing index (AAI) is derived from the change in the spectral dependence of backscattered UV radiance by aerosols relative to Rayleigh scattering in the 354–388 nm spectral range. The AAI was found to be a useful indicator of elevated concentrations of UV-absorbing aerosols, such as dust (Jethva and Toress 2011), taking a near-zero value for clouds and weakly absorbing aerosols and a positive value for desert aerosols (Huang et al. 2010). Aura observes the study area between 09:00 and 11:00 UTC with a nearly daily pass. Two years (1 January 2007–31 December 2008) of OMI AAI data (OM-AURA_L2) with spatial resolution of 13 km × 24 km were used.

3. Methods

Using half-hourly ground PM_{10} records from 2007 to 2008, we assembled a list of DD and NDD based on a modification of Ganor, Stupp, and Alpert's (2009) scheme for DD identification. Since dust events have a considerable spatial extent (Yuval and Broday 2006), we modified Ganor et al.'s scheme, requiring that the conditions for DD identification (see Section 1) occur in at least three nearby monitoring stations simultaneously (or within a very short lag time). The DD list was scrutinized using (a) HYSPLIT back-trajectories of the air masses, (b) Alpert et al.'s (2004) semi-objective synoptic classification, and (c) a careful inspection of the synoptic maps on the DD.

The differences between the two populations (DD and NDD) in seasonality, synoptic class frequency, daily average ground-monitoring parameters ($PM_{2.5}$, RH, etc.), and the SRS aerosol products were examined. The distinct differences between these two populations (see Section 4) supported the development of a DD/NDD classification model (Figure 2). As a first step, the best discrimination rules for distinguishing between DD and NDD were obtained using the nonparametric Classification and Regression Tree (CART) algorithm (Breiman et al. 1984). CART has been used to identify the potential causal relationships in a variety of environmental data sets (e.g. Hu et al. 2008; Rothwell, Futter, and Dise 2008; Sullivan et al. 2006). It has also been applied to the entire study database, which included a categorical seasonality variable (month) and daily SRS aerosol products: AOD, AE, and SSA (from MODIS) and AAI (from OMI). This database is designated hereafter as DB1. The binary response variable 'dust' takes the values $dust = 1$ for DD and $dust = 0$ for NDD. The output of this step was the best set of explanatory factors (rules) that were associated with $dust = 1$. These factors were used to transform DB1 into a binary database (DB2), which was used to develop a logistic regression model for identifying DD. The CART model was applied using 'R' software (R Development Core Team 2009). The CART algorithm can specify prior information to the outcome probabilities and use it for building the tree. We examined to what extent prior information on the 5 year mean ratio of DD/NDD in the study area ($\sim$1:10) modifies the CART selection of optimal factors for DD classification. A cross-validation procedure was applied for estimating the misclassification rates. The final partitioning of the data was determined using the tree that reveals the smallest cross-validation estimation error (Breiman et al. 1984).

Occurrence of DD ($dust = 1$) was modelled by a logistic regression of the form

$$\text{logit}\,(P) = \ln\left(\frac{P}{1-P}\right) = \beta_0 + \beta_1 x_1 + \beta_2 x_2 + \beta_3 x_3 + \beta_4 x_4, \tag{1}$$

where P is the probability of DD occurrence and the x's are the variables obtained by the CART (see Table 5). Equation (1) has been parameterized by regressing it against a training subset that was constructed by randomly selecting 80% of each population (DD and NDD) from DB2. Subsequently, evaluation of the logistic model was performed using a test subset, i.e. the remaining 20% of DB2. This procedure (i.e. model parameterization and evaluation) was repeated 10 times for 10 different random selections of the training and test data sets. For each record in the test subsets, the probability, P, that $dust = 1$ was calculated. Each observation in the test set was classified as a dust day if its calculated probability, P, was higher than a given threshold. This threshold was determined after examining the receiver operating characteristic (ROC) curves that were obtained for each run. Each point on the ROC curve represents a sensitivity/specificity pair that corresponds to a particular discrimination threshold (Bradely 1997; Fawcatt 2005; Zweig and Campbell 1993). It is

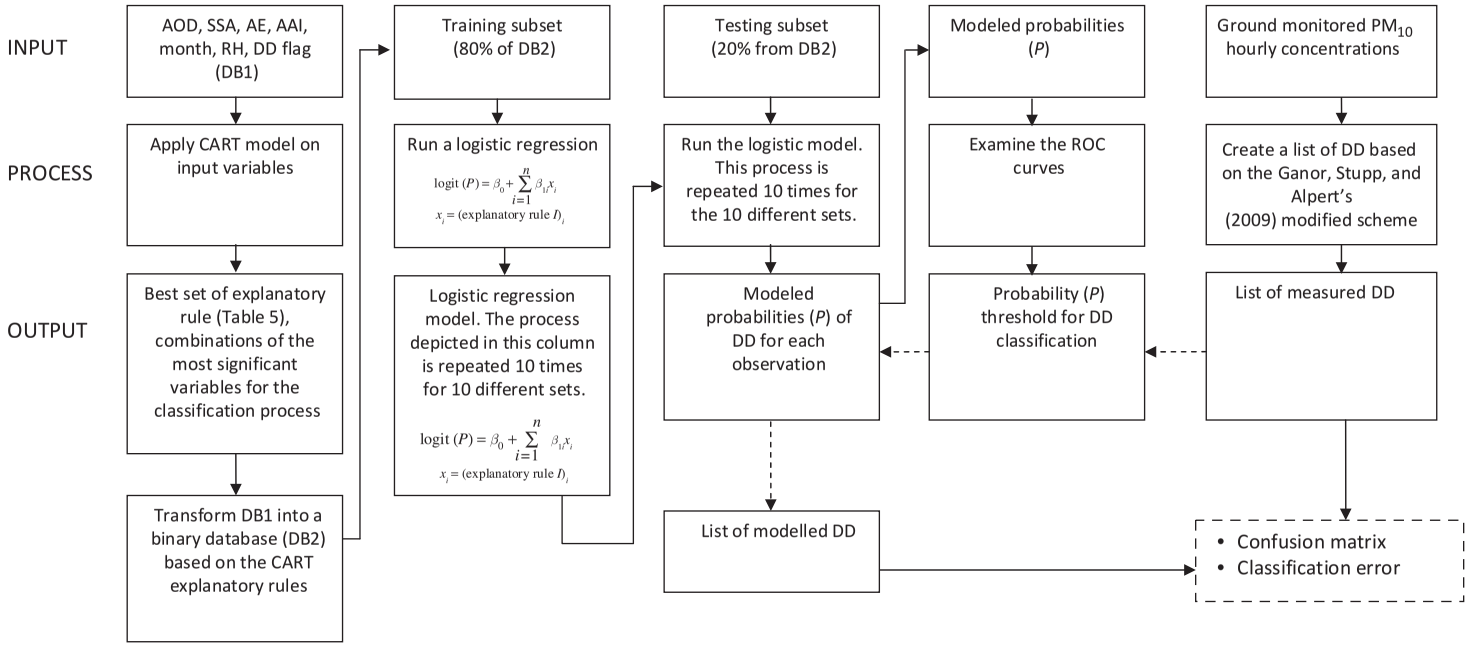

Figure 2. Flow chart of model variables, processes, and information transfer.

noteworthy that the true DD and NDD populations were obtained using Ganor, Stupp, and Alpert's (2009) modified scheme and served as the evaluation list against which the model could be tested. Since DD were found to be associated with certain RH profiles (Falkovich et al. 2004; Ganor et al. 2010), we examined also whether the use of surface RH data, if available, as an additional explanatory variable can improve the performance of the model.

4. Results

An analysis of the half-hourly ground PM_{10} monitoring data from January 2007 to December 2008 revealed 67 DD and 664 NDD. Most DD occurred in spring (March to May, 57%) and winter (December to February, 31%) in agreement with previous findings (Dayan and Levy 2005; Dayan et al. 2007; Erel et al. 2006). A meticulous analysis of synoptic maps for the DD supported our classification of the 67 DD using the modified Ganor scheme. Based on Alpert et al.'s (2004) semi-objective synoptic classification scheme, the synoptic distribution of these populations (Figure 3, Table 1) demonstrates that DD occurred mostly on days characterized by Sharav lows (cyclones that form along the North African and the southern Mediterranean coastline) and lows to the north and to the west (e.g. Cyprus lows), whereas Persian troughs and highs to the west were more common on NDD. However, neither DD nor NDD were characterized by one prevailing synoptic class. This conclusion holds also when the 19 synoptic classes are pooled into six dominant synoptic patterns (Red Sea trough, Persian trough, highs, winter lows, lows to the east, and Sharav low). It is noteworthy that since synoptic systems move more slowly than the measured winds, the synoptic classification may not be always synchronized with actual dust occurrences. This limits the applicability of synoptic classification for DD identification and prediction, especially if the dust event does not occur close to the synoptic classification time, i.e. 12:00 UTC. This conclusion is in general agreement with the findings of Dayan et al. (2007), Carmona and Alpert (2009), and Ganor et al. (2010).

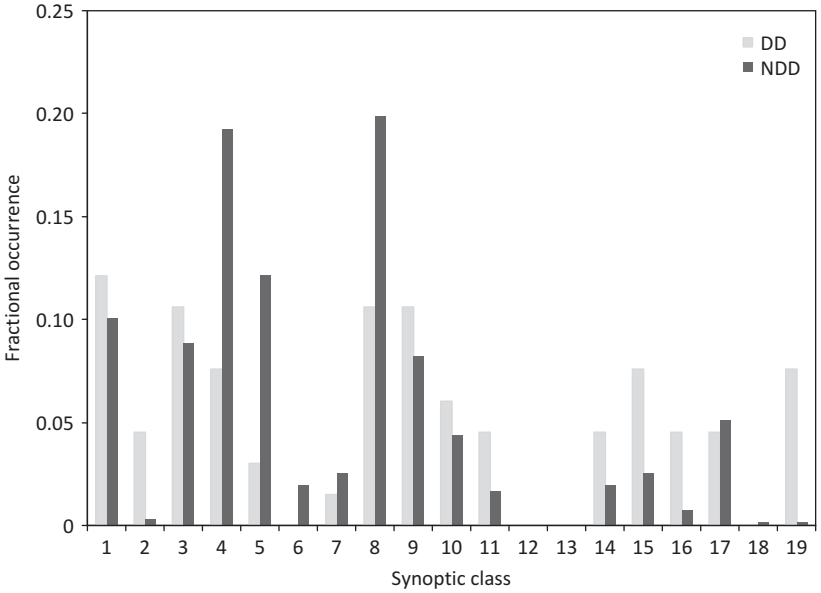

Figure 3. Distribution of DD and NDD by synoptic class in 2007–2008.

Table 1. Synoptic classes and their synoptic pattern category in the Eastern Mediterranean (following Alpert et al. 2004).

Synoptic class (with number)		Synoptic pattern (with number)	
1	Red Sea trough with eastern axis	I	Red Sea trough
2	Red Sea trough with western axis	I	Red Sea trough
3	Red Sea trough with central axis	I	Red Sea trough
4	Persian trough (weak)	II	Persian trough
5	Persian trough (medium)	II	Persian trough
6	Persian trough (deep)	II	Persian trough
7	High to the east	III	Highs
8	High to the west	III	Highs
9	High to the north	III	Highs
10	High over Israel (central)	III	Highs
11	Low to the east (deep)	IV	Low to the east
12	Cyprus low to the south (deep)	V	Winter lows
13	Cyprus low to the south (shallow)	V	Winter lows
14	Cyprus low to the north (deep)	V	Winter lows
15	Cyprus low to the north (shallow)	V	Winter lows
16	Cold low to the west	V	Winter lows
17	Low to the east (shallow)	IV	Low to the east
18	Sharav low to the west	VI	Sharav low
19	Sharav low over Israel (central)	VI	Sharav low

Studying the distribution of different ground-monitoring parameters in the two populations, Figure 4 depicts that the $PM_{2.5}/PM_{10}$ ratio has a significantly narrower range and a smaller median and mean on DD than on NDD (Table 2). Similar results were also observed in the Haifa Bay area, Israel, with mean $PM_{2.5}/PM_{10}$ ratios of 0.36 and 0.65 on DD and NDD, respectively (HDMAE 2008). This result supports previous findings that high background $PM_{2.5}$ concentrations (mainly sulphate transported from Eastern Europe) characterize NDD in the East Mediterranean, whereas DD are dominated by coarser size aerosols (Asaf et al. 2008). Table 2 reveals that the differences between DD and NDD populations are statistically significant. In particular, the difference in ambient RH between the two populations results from the lower RH of desert-borne air masses compared to the higher RH of air masses on NDD (Ganor et al. 2010).

Among the satellite-borne remotely sensed parameters studied, only AOD and AE showed significant differences between the two populations (Table 3), suggesting that these parameters may be useful for DD identification based on SRS aerosol products. However, it is notable that although DD and NDD were characterized as having a significantly different AE, its maximum value was lower than 1 in both populations even if $AE > 1$ could be expected on NDD. Moreover, although only marginal differences were observed in the SSA and the AAI between DD and NDD, the tails of their pertinent distributions (especially for the SSA) were different in the two populations (Figure 5). These observations demonstrate the difficulties when the input to the DD classification model is obtained by a subjective choice of variables.

Tables 2 and 3 and Figure 5 depict that DD are characterized by high variability of both ground and satellite-borne parameters, but that it may be possible to use SRS aerosol products for DD identification. However, relative to the continuous ground-monitoring data, AOD retrievals at any given location can be obtained only once or twice per day and require cloud-free conditions. In particular, the limited availability of the SSA (Table 4) during the study period severely affected the possibility of using it within a DD classification model.

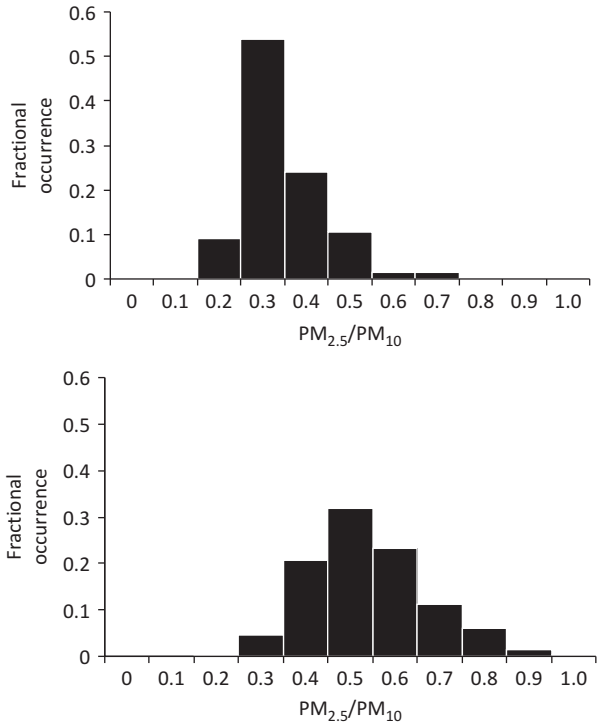

Figure 4. Ratio of ground $PM_{2.5}$ to PM_{10} concentrations on DD (top) and NDD (bottom) in southern Israel, 2007–2008.

Table 2. Statistics of daily mean ground-monitoring attributes on DD (67 cases) and NDD (664 cases) in the years 2007–2008.

	First−third quartiles		Median		
	DD	NDD	DD	NDD	*p*-Value*
PM_{10} ($\mu g\ m^{-3}$)	106.3–176.4	30.3–47.4	124.43	38.94	<0.001
$PM_{2.5}$ ($\mu g\ m^{-3}$)	28.7–49.5	14.2–23.7	36.48	18.79	<0.001
$PM_{2.5}/PM_{10}$	0.23–0.33	0.40–0.57	0.27	0.48	<0.001
RH	54.5–74.6	64.6–77.7	64	72.22	<0.001

Note: *Mann–Whitney test.

Table 3. Statistics of daily mean SRS parameters on DD (67 cases) and NDD (664 cases) in the years 2007–2008.

	First−third quartiles		Median		
	DD	NDD	DD	NDD	*p*-Value*
AOD	0.29–0.67	0.19–0.35	0.46	0.25	< 0.001
AE	0.55–0.62	0.60–0.63	0.59	0.62	< 0.001
SSA	0.91–0.93	0.91–0.94	0.92	0.93	0.09
AAI	0.93–1.76	0.86–1.57	1.38	1.22	0.07

Note: *Mann–Whitney test.

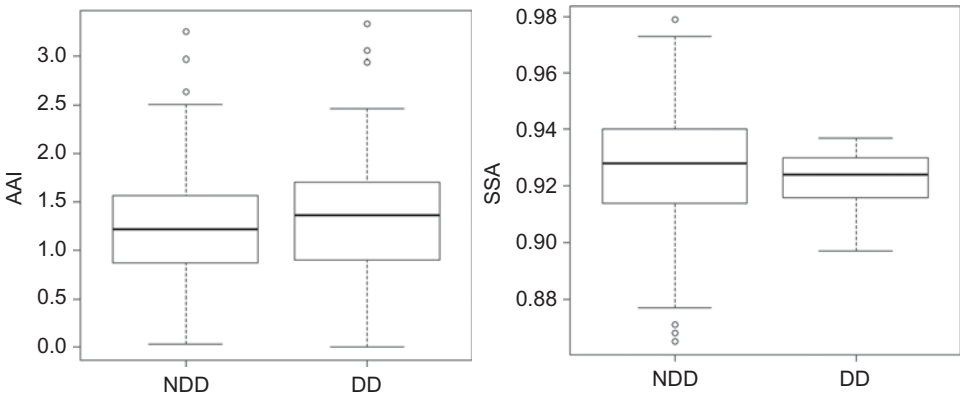

Figure 5. Box plots of the distribution of AAI (left) and SSA (right) on DD and NDD in the study area in 2007–2008.

Table 4. Availability of SRS aerosol product over the study area in 2007–2008.

			Data availability (%)		
Sensor	Algorithm	Retrieved parameters	All days	DD	NDD
MODIS (Terra and Aqua)	Dark target (DT)	Aerosol optical depth (AOD)	73	87	71
		Angstrom exponent (AE)	72	84	71
	Deep blue (DB)	Aerosol optical depth (AOD)	55	43	58
		Angstrom exponent (AE)	55	43	58
		Single scattering albedo (SSA)	20	22	20
OMI (Aura)		Aerosol absorbing index (AAI)	84	94	83

Table 5. CART model output 'rules' that characterize DD.

CART 'rules'	Month ≥ 6 AAI < 0.03	Month < 6 AOD ≥ 0.3160	Month ≥ 6 AOD ≥ 0.5636 AAI ≥ 0.03	Month < 4 $0.2077 \leq$ AOD < 0.3160
Parameter name in DB2	x_1	x_2	x_3	x_4

Note: The model uses only SRS aerosol products and the calendar month as input data (DB1).

Table 5 details the rules obtained when applying the CART model on DB1, i.e. when accounting for SRS aerosol products and the calendar month as the only potential explanatory variables for predicting the occurrence of ground-perceived DD. The four rules found by the CART algorithm were transformed into binary variables, x_i, $i = 1 \ldots 4$, and used in the logistic regression. Table 6 presents the results of one logistic regression (out of 10) based on one training subset of DB2. A pooled analysis of the 10 logistic regressions revealed that the probability, P, that $dust = 1$ is

$$\text{logit}\,(P) = -3.5 + 19.07x_1 + 2.65x_2 + 3.4x_3 + 1.85x_4. \quad (2)$$

The threshold $P = 0.47$ for the classification of DD was determined after examining the ROC curves that were produced for each of the 10 training sets. The area under these ROC curves ranged between 0.81–0.86, with a mean area of 0.83 (Figure 6).

Table 6. Results of a typical logistic regression (out of 10 independent runs) using a binary training subset of DB2.

	Coefficient	Standard error	*t*-Value	*P*
Intercept	−3.50	0.27	−12.91	<0.001
x_1	19.07	1029.10	0.02	0.98
x_2	2.65	0.74	3.58	<0.001
x_3	3.40	0.37	9.20	<0.001
x_4	1.85	0.56	3.32	<0.001

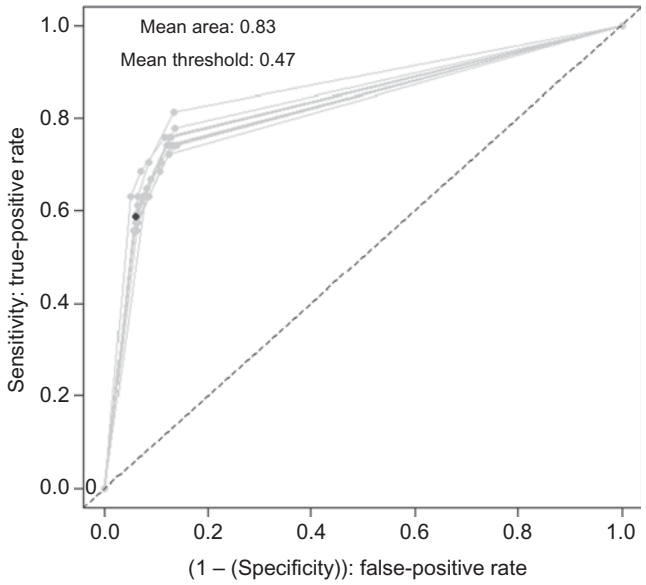

Figure 6. ROC curves of all 10 training sets of the logistic regression (Equation (2)). The black dot marks the mean true-positive (TP) and false-positive (FP) rates and corresponds to the mean optimal threshold value (0.47).

Based on the ground PM_{10} observations, the true fraction of DD in the study period was ∼9%. Since CART used this information throughout the construction of DB2, the naive prediction that all the days are NDD would have been wrong for ∼9% of the days. Table 7 displays a summary of the logistic regression model validation results. The prediction error has been calculated using equal fines for misclassification of either DD (i.e. false-negative) or NDD (i.e. false-positive).The prediction error represents the fraction of the observations that were wrongly classified during the evaluation procedure, with *B* and *C* representing the observations that were classified incorrectly as NDD and DD, respectively (*A* and *D* represent the correctly classified observations). As can be seen, the mean prediction error of the logistic regression model is 8.2%, with 94.7% and 61.5% correct classifications of NDD and DD, respectively. In fact, in 90% of the evaluation runs, the prediction error was smaller than 9% (the naive prediction). This demonstrates that the CART–logistic regression integrated model can predict well the occurrence of ground-level-perceived DD using the SRS aerosol products as model variables.

Since ambient RH was shown to differ significantly between DD and NDD (Table 2), we explored, following all the steps that were described earlier, whether incorporation of

Table 7. Statistics of the prediction error and the confusion matrix as obtained in the evaluation of the logistic regression model.

		True	
Predicted	NDD (0)		DD (1)
NDD (0)	*A*		*B*
DD (1)	*C*		*D*
Total	133		13

	Prediction error $\left(\frac{B+C}{A+B+C+D}\right)$	*A*	*B*	*C*	*D*
Minimum	0.062	120	3	4	6
First quartile	0.070	124	3	5	7
Median	0.082	126	5	7	9
Mean	0.082	126	5	7	8
Third quartile	0.082	128	6	9	10
Maximum	0.140	129	7	13	10

Note: Both model predictions and true observations are binary classified as NDD (0) or DD (1).

Table 8. Statistics of the prediction error and the confusion matrix of the alternative logistic regression model (i.e. with ground RH records included) as obtained in the evaluation process.

	Prediction error $\left(\frac{B+C}{A+B+C+D}\right)$	*A*	*B*	*C*	*D*
Minimum	0.027	123	0	4	6
First quartile	0.063	125	2	6	9
Median	0.072	126	4	7	10
Mean	0.068	126	3	7	10
Third quartile	0.081	127	4	8	11
Maximum	0.089	129	7	10	13

RH data into DB1 can improve the model predictions. As expected, the RH was found by CART to be a significant explanatory variable. An error analysis of this alternative model (Table 8) shows a mean prediction error of 6.8%, with 94.7% and 76.9% correct classifications of NDD and DD, respectively. Accounting for ground RH records improved the model's DD classification power by 15.4% (i.e. a 25% improvement relative to the base model) and yielded 93.2% correct classifications (the mean area under the ROC curves was 0.91, indicating a better model). All of the prediction errors during the evaluation runs of this alternative model were smaller than the baseline probability of DD (9%).

5. Discussion

The CART model results reveal that the most significant SRS aerosol product predictors of DD in southern Israel are the AOD and the AAI in agreement with Baddock, Bullard, and Bryant's (2009) findings in Australia. Incorporation of ambient RH data was found to significantly improve DD detection. Hence, if available, ambient RH data are recommended as an additional model variable, besides the month, the AOD, and the AAI. However, it should be emphasized that due to lack of dense spatial coverage of ground RH monitoring

in the study area, possible spatial RH variations could not be accounted for. Therefore, the model results presented in Table 8 need to be re-evaluated in areas with enhanced spatial coverage of RH measurements.

The AE was shown to significantly differ between DD and NDD (Table 3). Nonetheless, it did not turn out to be an important explanatory variable by the CART model. In contrast, the AAI differed only marginally between DD and NDD (Table 3), yet it was found by the CART to be a significant explanatory variable for DD classification. This probably results from the fact that the AE is derived from AOD retrievals at 470 and 670 nm; hence, the AE and the AOD are not independent of each other (e.g. retrieval of AE is not robust for low AOD). In contrast, since the AOD and the AAI represent distinct spectral signatures, they actually represent independent information and, thus, both were found useful for identification of DD. Whereas the information that the AAI carries in relation to DD identification may not be strong enough by itself (Table 3), when coupled with the information carried by the AOD, it has merit, as is evident from the CART output. In fact, the results of the CART model (Table 5) demonstrate that the optimal factors correspond to combinations of SRS aerosol products. These mixed factors are better predictors of DD than the factors that correspond to any single SRS aerosol product, very much like eigenvectors obtained by a principal component analysis.

To further assess the model, we evaluated it for the same years (2007–2008) using data from a different geographical area (Gush Dan, central Israel), which is nonetheless expected to be affected by the same dust events. Specifically, the model that has been developed and parameterized for southern Israel was applied for central Israel using SRS aerosol products over this region. To assess the model performance, its predictions were compared to a DD classification obtained using the modified Ganor scheme (see Section 3) by taking into account the ground PM_{10} data from stations in the Gush Dan area. Table 9 reveals that the model performed equally well in the two geographical areas. A similar mean correct classification of DD and NDD was obtained in both regions for the matched cases (B and E, D and F). It should be also further emphasized that, if available, ground RH data and prior information on the long-term DD/NDD ratio improve the model prediction power. Nonetheless, applying the model in regions other than the geographical area for which it has been developed should be done with care.

Table 9. Comparison of model evaluation results for southern and central Israel.

	Area	Ground RH	Prior information (DD/NDD ratio)	Mean correct classification (%)	
				DD	NDD
A	South Israel	−	+	61.5	94.7
B	South Israel	+	+	76.9	94.7
C	South Israel	−	−	23.1	100
D	South Israel	+	−	30.7	100
E	Gush Dan	+	+	71.2	89.5
F	Gush Dan	+	−	39.0	97.4

Notes: The models were developed and parameterized for southern Israel and either make use (+) or do not make use (–) of ground RH data and of prior information on the long-term DD/NDD ratio. According to the modified Ganor scheme for DD classification (see Section 3), in the years 2007–2008, southern Israel experienced 67 DD and 664 NDD, whereas central Israel experienced 64 DD and 666 NDD (the difference in the total number of days is due to data availability).

6. Conclusions

This work demonstrates the possibility to identify DD and NDD retrospectively using an objective statistical model with SRS aerosol products as input. The variables of the logistic regression prediction model were objectively selected by a CART model. The optimal variables of the logistic regression model are different combinations of the primary variables: the calendar month, the AOD, and the AAI. When the ground RH data are available and/or when the long-term DD/NDD ratio is known, including these data improves the model performance significantly. It is noteworthy that the hybrid nature of the factors that were selected by the CART as input variables to the logistic regression model, rather than using the individual physical variables by themselves as often done when regressing SRS aerosol products against ground PM, improves the overall model prediction.

We believe that a reliable partitioning of days into DD and NDD as perceived at the ground can be valuable in many research areas, particularly for environmental health studies where the impact of exposure to dust and non-dust PM may have distinct effects on our health. Indeed, the literature reveals a plethora of associations (in terms of relative risks) between a spectrum of adverse health effects and exposure to PM of mineralogical composition or from combustion processes. The approach proposed in this study may enable identification of two subpopulations of days, which can be used to study the pertinent effects of exposure to PM from distinct sources. Thus, this approach may possibly be used to develop more advanced epidemiological models and to enhance our understanding of health effects of particles of distinct composition. In particular, due to the vast spatial availability of SRS aerosol products, such a model may open the way to perform epidemiological studies in areas with limited ground air quality monitoring.

Acknowledgements

MSH was supported by scholarships from the Israel Ministry of Science and Technology and from the Israel Council for Higher Education. Data were obtained from the Goddard Earth Science Data Center in NASA GSFC, Israel Ministry of Environment Protection, Israel Electric Company, and the Ashdod-Ashkelon Association of Municipalities for the Environment. The study was done within the Technion Center of Excellence in Exposure Science and Environmental Health (TCEEH).

References

Alpert, P., S. O. Krichak, M. Tsidulko, H. Shafir, and J. H. Joseph. 2002. "A Dust Prediction System with TOMS Initialization." *Monthly Weather Review* 130: 2335–45.

Alpert, P., I. Osetinsky, B. Ziv, and H. Shafir. 2004. "Semi-Objective Classification for Daily Synoptic Systems: Application to the Eastern Mediterranean Climate Change." *International Journal of Climatology* 24: 1001–11.

Asaf, D., D. Pedersen, M. Peleg, V. Matveev, and M. Luria. 2008. "Evaluation of Background Levels of Air Pollutants over Israel." *Atmospheric Environment* 42: 8453–63.

Badarinath, K. V. S., S. K. Kharol, D. G. Kaskaoutis, A. R. Sharma, V. Ramaswamy, and H. D. Kambezidis. 2010. "Long-Range Transport of Dust Aerosols over the Arabian Sea and Indian Region – A Case Study Using Satellite Data and Ground-Based Measurements." *Global and Planetary Change* 72: 164–81.

Baddock, M. C., J. E. Bullard, and R. G. Bryant. 2009. "Dust Source Identification Using MODIS: A Comparison of Techniques Applied to the Lake Eyre Basin, Australia." *Remote Sensing of Environment* 113: 1511–28.

Bradely, A. P. 1997. "The Use of the Area under the ROC Curve in the Evaluation of Machine Learning Algorithms." *Pattern Recognition* 30: 1145–59.

Breiman, L., J. H. Friedman, R. A. Olshen, and C. J. Stone. 1984. *Classification and Regression Trees*. Monterey, CA: Wadsworth & Brooks/Cole Advanced Books & Software.

Carmona, I., and P. Alpert. 2009. "Synoptic Classification of Moderate Resolution Imaging Spectroradiometer Aerosols over Israel." *Journal of Geophysical Research* 114: 1–15.
Christopher, S. A., and T. A. Jones. 2010. "Satellite and Surface-Based Remote Sensing of Saharan Dust Aerosols." *Remote Sensing of Environment* 114: 1002–7.
Dayan, U., and I. Levy. 2005. "The Influence of Meteorological Conditions and Atmospheric Circulation Types on PM10 and Visibility in Tel Aviv." *Journal of Applied Meteorology* 44: 606–19.
Dayan, U., B. Ziv, T. Shooba, and Y. Enzela. 2007. "Suspended Dust over the Southeastern Mediterranean and Its Relation to Atmospheric Circulations." *International Journal of Climatology* 28: 915–24.
Engel-Cox, J. A., C. H. Holloman, B. W. Coutant, and R. M. Hoff. 2004. "Qualitative and Quantitative Evaluation of MODIS Satellite Sensor Data for Regional and Urban Scale Air Quality." *Atmospheric Environment* 38: 2495–509.
Erel, Y., U. Dayan, R. Rabi, Y. Rudich, and M. Stein. 2006. "Trans Boundary Transport of Pollutants by Atmospheric Mineral Dust." *Environmental Science and Technology* 40: 2996–3005.
Falkovich, A. H., G. Schkolnik, E. Ganor, and Y. Rudich. 2004. "Adsorption of Organic Compounds Pertinent to Urban Environments onto Mineral Dust Particles." *Journal of Geophysical Research* 109: D02208.
Fawcatt, T. 2005. "An Introduction to ROC Analysis." *Pattern Recognition Letters* 27: 861–74.
Ganor, E., A. Stupp, and P. Alpert. 2009. "A Method to Determine the Effect of Mineral Dust Aerosols on Air Quality." *Atmospheric Environment* 43: 5463–8.
Ganor, E., A. Stupp, I. Osetinsky, and P. Alpert. 2010. "Synoptic Classification of Lower Troposphere Profiles for Dust Days." *Journal of Geophysical Research* 115: 1–8.
Goudie, A. S., and N. J. Middleton. 2006. *Desert Dust in the Global System*. Heidelberg: Springer.
Haifa District Municipal Association for Environmental Protection (HDMAE). 2008. Annual Report. Accessed December 1, 2012. Hebrew, http://www.envihaifa.org.il/.
Hoff, R. M., and S. A. Christopher. 2009. "Remote Sensing of Particulate Pollution from Space: Have We Reached the Promised Land?" *Journal of the Air and Waste Management Association* 59: 645–75.
Hu, W., K. L. Mengersen, A. J. McMichael, and S. Tong. 2008. "Temperature, Air Pollution and Total Mortality during Summers in Sydney, 1994–2004." *International Journal of Biometeorology* 52: 689–96.
Hu, Z. 2009. "Spatial Analysis of MODIS Aerosol Optical Depth, $PM_{2.5}$, and Chronic Coronary Heart Disease." *International Journal of Health Geographics* 8: 27–36.
Hu, Z., and K. R. Rao. 2009. "Particulate Air Pollution and Chronic Ischemic Heart Disease in the Eastern United States: A County Level Ecological Study Using Satellite Aerosol Data." *Environmental Health* 8: 26–35.
Huang, J., P. Minnis, H. Yan, Y. Yi, B. Chen, L. Zhang, and J. K. Ayers. 2010. "Dust Aerosol Effect on Semi-Arid Climate over Northwest China Detected from A-Train Satellite Measurements." *Atmospheric Chemistry and Physics* 10: 6863–72.
Hutchison, K. D., S. Smith, and S. J. Faruqui. 2005. "Correlating MODIS Aerosol Optical Thickness Data with Ground-Based PM2.5 Observations across Texas for Use in a Real-Time Air Quality Prediction System." *Atmospheric Environment* 39: 7190–203.
Ichoku, C., D. A. Chu, S. Mattoo, Y. J. Kaufman, L. A. Remer, D. Tanre, I. Slutsker, and B. N. Holben. 2002. "A Spatio-Temporal Approach for Global Validation and Analysis of MODIS Aerosol Products." *Geophysical Research Letters* 29: 1–4.
Jethva, H., and O. Torres. 2011. "Satellite-Based Evidence of Wavelength-Dependent Aerosol Absorption in Biomass Burning Smoke Inferred from Ozone Monitoring Instrument." *Atmospheric Chemistry and Physics Discussions* 11: 7291–319.
Jiménez, E., C. Linares, D. Martínez, and J. Díaz. 2010. "Role of Saharan Dust in the Relationship between Particulate Matter and Short-Term Daily Mortality among the Elderly in Madrid (Spain)." *Science of the Total Environment* 408: 5729–36.
Kalderon-Asael, B., Y. Erel, A. Sandler, and U. Dayan. 2009. "Mineralogical and Chemical Characterization of Suspended Atmospheric Particles over the East Mediterranean Based on Synoptic-Scale Circulation Patterns." *Atmospheric Environment* 43: 3963–70.
Kaskaoutis, D. G., H. D. Kambezidis, N. Hatzianastassiou, P. G. Kosmopoulos, and K. V. S. Badarinath. 2007. "Aerosol Climatology: On the Discrimination of Aerosol Types over Four AERONET Sites." *Atmospheric Chemistry and Physics Discussions* 7: 6357–411.

Kaufman, Y. J., B. N. Holben, D. Tanre, I. Slutsker, A. Smirnov, and T. F. Eck. 2000. "Will Aerosol Measurements from Terra and Aqua Polar Orbiting Satellites Represent the Daily Aerosol Abundance and Properties?" *Geophysical Research Letters* 27: 3861–4.

Kaufman, Y. J., I. Koren, L. A. Remer, D. Tanre, P. Ginoux, and S. Fan. 2005. "Dust Transport and Deposition Observed from the Terra Moderate Resolution Imaging Spectroradiometer (MODIS) Spacecraft Over the Atlantic Ocean." *Journal of Geophysical Research* 110: 1–16.

Kazadzis, S., A. Bais, A. Arola, N. Krotkov, N. Kouremeti, and C. Meleti. 2009. "Ozone Monitoring Instrument Spectral UV Irradiance Products: Comparison with Ground Based Measurements at an Urban Environment." *Atmospheric Chemistry and Physics* 9: 585–94.

Laden, F., L. M. Neas, D. W. Dockery, and J. Schwartz. 2000. "Association of Fine Particulate Matter from Different Sources with Daily Mortality in Six U.S. Cities" *Environmental Health Perspectives* 108: 941–7.

Lee, H. J., Y. Liu, B. A. Coull, J. Schwartz, and P. Koutrakis. 2011. "A Novel Calibration Approach of MODIS AOD Data to Predict PM2.5 Concentrations." *Atmospheric Chemistry and Physics Discussions* 11: 9769–95.

Levy, R. C., L. A. Remer, R. G. Kleidman, S. Mattoo, C. Ichoku, R. Kahn, and T. F. Eck. 2010. "Global Evaluation of the Collection 5 MODIS Dark-Target Aerosol Products over Land." *Atmospheric Chemistry and Physics Discussions* 10: 14815–73.

Levy, R. C., L. A. Remer, D. Tanré, S. Mattoo, and Y. J. Kaufman. 2009. "Algorithm for Remote Sensing of Tropospheric Aerosol over Dark Targets from MODIS: Collections 005 and 051 Revision 2." Accessed December 1, 2012. http://modis-atmos.gsfc.nasa.gov/_docs/ATBD_MOD04_C005_rev2.pdf.

Lipsett, M. J., F. C. Tsai, L. Roger, M. Woo, and B. D. Ostro. 2006. "Coarse Particles and Heart Rate Variability among Older Adults with Coronary Artery Disease in the Coachella Valley, California." *Environmental Health Perspectives* 114: 1215–20.

Martin, R. V. 2008. "Satellite Remote Sensing of Surface Air Quality." *Atmospheric Environment* 42: 7823–43.

Meloni, D., A. Di Sarra, G. Pace, and F. Monteleone. 2006. "Aerosol Optical Properties at Lampedusa (Central Mediterranean), 2. Determination of Single Scattering Albedo at Two Wavelengths for Different Aerosol Type." *Atmospheric Chemistry and Physics* 6: 715–27.

Metz, C. E. 1978. "Basic Principles of ROC Analysis." *Seminars in Nuclear Medicine* 8: 283–98.

Middleton, N., P. Yiallouros, S. Kleanthous, O. Kolokotroni, J. Schwartz, D. W. Dockery, P. Demokritou, and P. Koutrakis. 2008. "A 10-Year Time-Series Analysis of Respiratory and Cardiovascular Morbidity in Nicosia, Cyprus: The Effect of Short-Term Changes in Air Pollution and Dust Storms." *Environmental Health* 7: 39–54.

Ochirkhuyag, L., and R. Tsolmon. 2008. "Monitoring the Source of Trans-National Dust Storms in Northeast Asia." In Proceedings of 21st ISPRS Congress, Beijing, China.

Pacioreck, C. J., Y. Liu, H. Moreno-Macias, and S. Kondragunta. 2008. "Spatiotemporal Associations between GOES Aerosol Optical Depth Retrievals and Ground-Level $PM_{2.5}$." *Environmental Science and Technology* 42: 5800–6.

Prospero, J. M., E. Blades, R. Naidu, G. Mathison, H. Thani, and M. C. Lavoie. 2008. "Relationship Between African Dust Carried in the Atlantic Trade Winds and Surges in Pediatric Asthma Attendances in the Caribbean." *International Journal of Biometeorology* 52: 823–32.

R Development Core Team. 2009. *R: A Language and Environment for Statistical Computing*. Vienna: R Foundation for Statistical Computing. Accessed December 1, 2012. http://www.R-project.org.

Rothwell, J. J., M. N. Futter, and N. B. Dise. 2008. "A Classification and Regression Tree Model of Controls on Dissolved Inorganic Nitrogen Leaching from European Forests." *Environmental Pollution* 156: 544–52.

Rudich, Y., Y. J. Kaufman, U. Dayan, H. Yu, and R. G. Kleidman. 2008. "Estimation of Transboundary Transport of Pollution Aerosols by Remote Sensing in the Eastern Mediterranean." *Journal of Geophysical Research* 113: 1–8.

Schwartz, J., G. Norris, T. Larson, L. Sheppard, C. Claiborn, and J. Koenig. 1999. "Episodes of High Coarse Particle Concentrations Are Not Associated with Increased Mortality." *Environmental Health Perspectives* 107: 339–42.

Stammes, P., and R. Noordhoek. 2002. "OMI Algorithm Theoretical Basis Document, Volume III, Clouds, Aerosols, and Surface UV Irradiance." Accessed December 1, 2012. http://eospso.gsfc.nasa.gov/eos_homepage/for_scientists/atbd/docs/OMI/ATBD-OMI-03.pdf.

Sullivan, M. S., M. J. Jones, D. C. Lee, S. J. Marsden, A. H. Fielding, and E. Young. 2006. "A Comparison of Predictive Methods in Extinction Risk Studies: Contrasts and Decision Trees." *Biodiversity and Conservation* 15: 1977–91.

Van Donkelaar, A., R. V. Martin, M. Brauer, R. Kahn, R. C. Levy, C. Verduzco, and P. J. Villeneuve. 2010. "Global Estimates of Ambient Fine Particulate Matter Concentrations from Satellite-Based Aerosol Optical Depth: Development and Application." *Environmental Health Perspectives* 118: 847–55.

Van Donkelaar, A., R. V. Martin, R. C. Levy, A. M. Da Silva, M. Krzyzanowski, N. E. Chubarova, E. Semutnikova, and A. J. Cohen. 2011. "Satellite-based Estimates of Ground-level Fine Particulate Matter During Extreme Events: A Case Study of the Moscow Fires in 2010." *Atmospheric Environment* 45: 6225–32.

Washington, R., M. Todd, N. J. Middleton, and A. S. Goudie. 2003. "Dust-Storm Source Areas Determined by the Total Ozone Monitoring Spectrometer and Surface Observations." *Annals of the Association of American Geographers* 93: 297–313.

Yuval, and D. M. Broday. 2006. "High-Resolution Spatial Patterns of Long-Term Mean Concentrations of Air Pollutants in Haifa Bay Area." *Atmospheric Environment* 40: 3653–64.

Zweig, M. H., and G. Campbell. 1993. "Receiver-Operating Characteristic (ROC) Plots: A Fundamental Evaluation Tool in Clinical Medicine." *Clinical Chemistry* 39: 561–77.